N_2O decomposition over liquid ion-exchanged Fe-BEA catalysts: correlation between activity and the IR intensity of adsorbed NO at 1874 cm^{-1}

G. Mul[a,*], M.W. Zandbergen[a], F. Kapteijn[a], J.A. Moulijn[a], and J. Pérez-Ramírez[a,b]

[a]*Reactor and Catalysis Engineering, DelftChemTech, Delft University of Technology, Julianalaan 136, 2628 BL, Delft, The Netherlands*
[b]*Norsk Hydro, Agri Research Centre, Nitric Acid Technology, P.O. Box 2560, N-3907 Porsgrunn, Norway*

Received 4 December 2003; accepted 16 December 2003

Various Fe-BEA catalysts have been synthesized by liquid ion-exchange, varying the iron precursor (nitrate, sulfate or chloride), the iron content (0.2–1.5 wt% Fe), and the conditions of activation, i.e. atmosphere (air or inert) and heating rate (5 or 20 K min^{-1}). The catalysts were tested in direct N_2O decomposition in the temperature range of 625–825 K. An optimal iron loading of 0.8 wt% Fe was found, with no significant influence of the used Fe-precursor. Activation of the ion-exchanged catalysts in inert gas yields significantly better performance than activation in air. NO adsorption combined with infrared analysis was used to characterize the various Fe^{2+} species present in the differently prepared Fe-BEA zeolites. A correlation exists between the absorption intensity of NO at 1874 cm^{-1} and the activity of the catalysts in N_2O decomposition. This relationship, which can be used as a reliable and fast assessment of catalyst performance, suggests an important role of ferrous ions in the activity of these catalysts. Based on these results and previous mechanistic studies using transient techniques, the NO absorption band at 1874 cm^{-1} is tentatively assigned to oligonuclear oxocations in the zeolite channels, with general formula Fe_xO_y.

KEY WORDS: N_2O decomposition; Fe-BEA; preparation; ion exchange; iron form; oligonuclear species; isolated species; infrared spectroscopy; NO adsorption.

1. Introduction

Fe-zeolites gained a great interest because of their excellent performance in many different catalytic conversions, e.g., direct N_2O decomposition [1–3], selective catalytic reduction (SCR) of NO_x and N_2O-SCR with hydrocarbons or ammonia [4–6], selective oxidation of NH_3 to N_2 with O_2 [7], N_2O-mediated selective oxidation of benzene to phenol [8,9], and more recently oxidative dehydrogenation of propane to propene with N_2O [10]. Many research groups have aimed at investigating the structure–activity relationship of these catalysts, particularly the effect of the preparation procedure on the nature of (active) iron species and the associated catalytic performance [11–16]. It is interesting to note, however, that most of these studies have applied MFI and particularly ZSM-5 as the host for Fe, while other zeolite types have been much less frequently investigated. Zeolite beta (BEA) appears to be an attractive host for iron in view of the various works by Coq *et al.* [6,17–21], who reported a superior performance of liquid ion-exchanged Fe-BEA in direct N_2O decomposition and SCR of N_2O by ammonia, compared to Fe-ZSM-5. Also Kameoka *et al.* [22,23] concluded that for the SCR of N_2O with CH_4 in the presence of excess oxygen, Fe-BEA showed a much higher activity per iron site (turnover frequency) than FeMFI catalysts, both prepared by liquid-ion exchange with $FeSO_4$. The effect of the preparation procedure on the performance of Fe-BEA catalysts has been less extensively evaluated as compared to FeMFI catalysts. Moreover, to the best of our knowledge, no reports exist on IR characterization, using adsorbed NO, of the Fe-sites in BEA zeolite. In view of the promising performance of the latter system, research in this direction is of interest for catalyst optimization.

In this paper, liquid-ion-exchanged Fe-BEA catalysts have been synthesized, characterized, and tested in direct N_2O decomposition. Several preparation steps have been varied, including the iron precursor and loading and the activation conditions (atmosphere and heating rate). NO adsorption combined with infrared spectroscopy has been applied in order to determine the form, location, and dynamic behavior of the iron species in the differently prepared zeolites. A remarkable correlation has been derived between the catalytic activity in N_2O decomposition and the intensity of an NO absorption band at around 1874 cm^{-1}. The assignments of the different infrared bands are discussed.

2. Experimental

2.1. Catalyst preparation

An overview of all the prepared catalysts used for the present study, including the nomenclature and the

---

[*] To whom correspondence should be addressed.
E-mail: g.mul@tnw.tudelft.nl

Table 1
Fe-BEA catalysts prepared in this study

Catalyst	Ion-exchange[a]		Activation[b]		
	Precursor	Atmosphere	Δr^{c}/K min^{-1}	Loading/wt% Fe	
				Nominal	In solid[d]
Fe-BEA(1)	$FeSO_4 \cdot 7H_2O$	Ar	5	0.8	0.72
Fe-BEA(2)	$FeCl_2$	Ar	5	0.8	0.69
Fe-BEA(3)	$Fe(NO_3)_3 \cdot 9H_2O$	Ar	5	0.8	0.74
Fe-BEA(4)	$FeSO_4 \cdot 7H_2O$	Air	5	0.8	0.71
Fe-BEA(5)	$Fe(NO_3)_3 \cdot 9H_2O$	Air	5	0.8	0.75
Fe-BEA(6)	$Fe(NO_3)_3 \cdot 9H_2O$[e]	Ar	5	0.8	0.78
Fe-BEA(7)	$Fe(NO_3)_3 \cdot 9H_2O$	Ar	20	0.8	0.74
Fe-BEA(8)	$Fe(NO_3)_3 \cdot 9H_2O$	Ar	5	0.2	0.19
Fe-BEA(9)	$Fe(NO_3)_3 \cdot 9H_2O$	Ar	5	1.5	1.43

[a] Liquid (aqueous) ion-exchange at room temperature for 20 h.
[b] Activation at 773 K in 100 mL STP min^{-1} of air or argon for 5 h.
[c] Heating rate during activation.
[d] Determined by ICP-OES.
[e] Ar was bubbled during the suspension during the ion exchange.

preparation variables, is presented in table 1. Typically, the following procedure was used in the ion-exchange method: 2 g of commercial NH_4-BEA zeolite (CP814E, Zeolyst, Si/Al = 11.5) was suspended in 300 mL water in a 1 L teflon flask. Appropriate amounts of iron precursors, $Fe(NO_3)_3 \cdot 9H_2O$ (>99.0%, Acros), $FeSO_4 \cdot 7H_2O$, >99.0%, J.T. Baker), or $FeCl_2$ (>99.5%, Alfa Aegar), corresponding to nominal iron loadings of 0.2, 0.8, and 1.5 wt% Fe, were weighed and dissolved in 100 mL of water, and added to the suspension. An additional amount of 600 mL of water was added to the flask. The pH of the obtained suspension was adjusted to four during the ion-exchange process by addition of diluted acid, with the anion corresponding to the used Fe-precursor. Ion exchange was carried out at room temperature during 20 h, by continuous agitation of the suspension using automated shaking of the vessel. In one of the preparations, Ar bubbling through the solution was present during the entire exchange procedure. After the ion exchange procedure, the samples were filtered, washed with deionized water, and dried at 373 K overnight. Finally, these samples were activated in a fixed-bed reactor, using flowing argon or air (100 mL STP min^{-1}) at 773 K for 5 h. Temperature ramps of 5 and 20 K min^{-1} were applied. Chemical composition of the final catalysts was determined by ICP-OES (Perkin-Elmer Plasma 40 (Si) and Optima 3000DV (axial)).

2.2. Catalyst testing

Activity measurements were carried out in a six-flow reactor system [24], using 50 mg of catalyst (125–200 μm) and a space time of 8.65×10^5 g s mol^{-1}. The space time is defined as the ratio $W/F(N_2O)_o$, where W is the catalyst mass and $F(N_2O)_o$ the molar flow of N_2O at the reactor inlet. The feed composition was 4.5 mbar N_2O in He at 3 bar of total pressure in each reactor. Before reaction, the catalysts were pretreated in He at 723 K for 1 h and cooled down to the initial reaction temperature. This was followed by exposure of the catalyst to the reaction mixture. The temperature was increased at intervals of 25 K in the range of 625–825 K. This cycle was followed by a stepwise decrease of temperature in 25 K steps. In this temperature range deactivation of the catalysts was absent and up and downcycles lead to very similar activity curves. Application of relevant criteria [24] under the experimental conditions revealed that mass and heat transport limitations in the catalyst at a particle level were absent.

N_2O, N_2, and O_2 were analyzed with a GC (Chrompack CP 9001) equipped with a thermal conductivity detector, using a Poraplot Q column (for N_2O separation) and a Molsieve 5A column (for N_2 and O_2 separation). At least three measurements in steady state were averaged for every activity data point. The N_2O conversion was calculated from the amount of N_2 formed. The mass balances for N and O closed at 99% and 98%, respectively.

2.3. Infrared characterization of NO adsorption

The location and form of the iron species in the different catalysts was determined by adsorption of NO in combination with FT-IR spectroscopy. The FT-IR measurements were performed using a Spectra-Tech DRIFT *in situ* high temperature cell (Diffuse Reflectance Infrared Fourier Transform), with CaF_2 windows. Ca. 25 mg were required to fill the ceramic cup of the DRIFT accessory. A mixture of 5 vol% NO in He (>99.998%) was fed to the cell using a 4-way valve (Valco), which was configured to select two separate gas feeds. A volummetric flow of 30 mL STP min^{-1} was

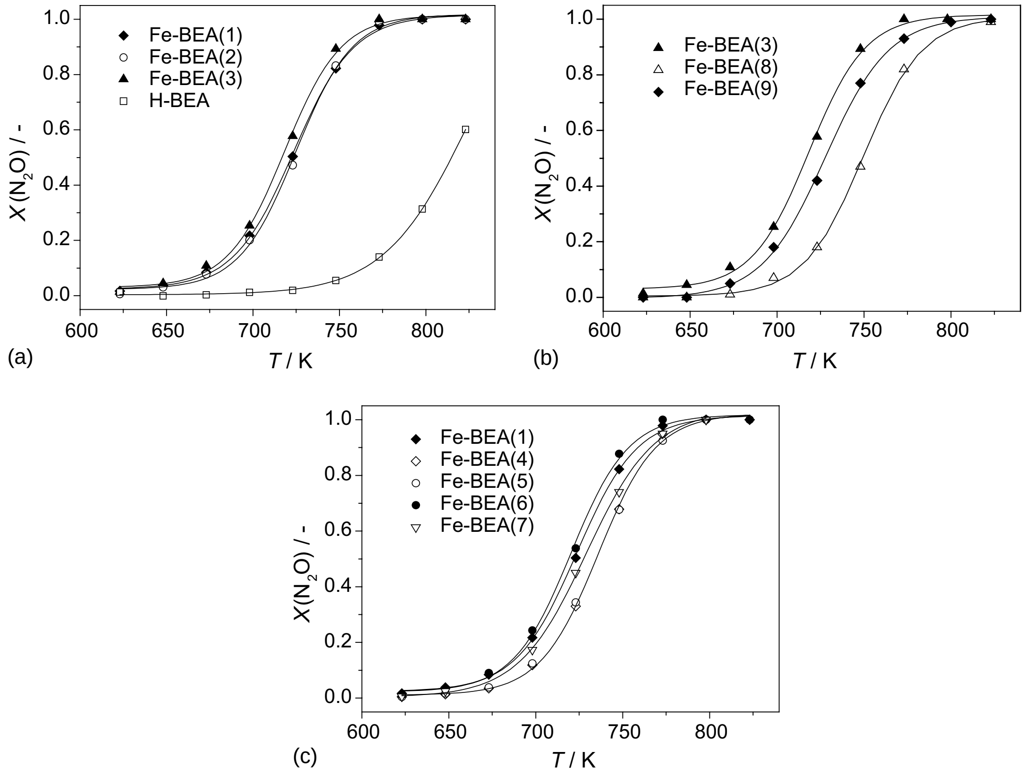

Figure 1. N_2O conversion versus T over liquid-ion-exchanged Fe-BEA catalysts prepared using different iron precursors (a), iron loadings (b), and activation procedures (c). Testing conditions: 4.5 mbar N_2O in He, $W/F(N_2O)_o = 8.65 \times 10^5$ g s mol^{-1}, $P = 3$ bar. See table 1 for catalyst codes.

used. Pretreatment of the powdered catalyst consisted of drying in He at 673 K for 60 min. The He gas feed (purity > 99.998%) was dried before use over a molecular sieve column. Spectra were recorded using a Nicolet Magna IR 860 spectrometer equipped with a nitrogen cooled MCT detector. Unless stated otherwise, spectra were recorded against a background of the sample at 323 K after pretreatment, at 4 cm^{-1} resolution, using co-addition of 64 scans. Spectra of the different catalysts are compared in absorption reflection units after 4 min exposure time to the 5 vol% NO in He and substraction of the gas-phase NO spectrum. The intensity of the respective absorption bands was calculated after a fitting procedure using GRAMS™ software, allowing a mixed Gaussian and Laurentzian peak shape. The error in the intensity of the 1874 cm^{-1} band is mainly induced by this fitting procedure, and estimated to be about 5% of the absolute value. Variations in NO pressure can be excluded to effect the spectra as a premix of NO in He was used, while also care was taken to use the spectra of equilibrated samples of similar quantities.

3. Results

3.1. Catalytic activity

Table 1 shows the ion-exchanged Fe-BEA samples used in this study and the variables of the preparations. The iron content in the catalysts was very similar to the nominal iron contents, which shows that the preparation procedure applied was effective. The influence of the iron precursor, iron loading, and activation conditions on the N_2O decomposition activity is shown in figure 1. The precursor salt used to incorporate iron in the zeolite matrix has very little influence on the performance of the final Fe-BEA catalysts, as shown in figure 1(a). The catalyst prepared using iron(III) nitrate (Fe-BEA(3)) shows a slightly higher activity than those prepared using iron(II) sulfate (Fe-BEA(1)) and iron(II) chloride (Fe-BEA(2)). Concluding, no significant impact of potentially remaining counter-anionic species or of resulting differences in the oxidation state of iron in the final catalysts can be observed. The activity of Fe-BEA(6), prepared with Ar bubbling through the suspension during the ion exchange, was very similar to catalyst Fe-BEA(3). The activity of H-BEA, resulting from calcination of the parent sample at 823 K for 5 h is much lower than that of Fe-BEA catalysts, requiring ca.150 K higher temperature to achieve similar N_2O conversions. The Fe content in this zeolite was below the accuracy of the ICP-OES method applied (<500 ppm Fe) and indicates the essential role of iron in the catalyst to achieve high activities.

The effect of the Fe-content on the activity is also illustrated in figure 1b for the nitrate-based catalysts. FeBEA(5), containing 0.8 wt% Fe, exhibits the highest absolute N_2O conversion. The activity largely increases upon increasing the iron content from 0.2 to 0.8 wt% Fe. However, further increasing to 1.5 wt% is detrimental to the performance. The activation energy of the catalyst containing 0.2 and 0.8 wt% Fe (180 kJ mol^{-1}) was significantly higher than that of the catalyst containing 1.5 wt% Fe (150 kJ mol^{-1}). Apparent activation energies were estimated around the inflection (50% conversion) of the conversion versus temperature curves by assuming a plug-flow model and a first-order reaction in N_2O.

The activation procedure of the ion-exchanged samples also influences the catalyst performance (figure 1c). A relatively large negative effect on the catalytic activity is observed if the catalysts are pretreated in air (open symbols) instead of inert (Ar). As expected, the negative effect is independent on the iron precursor used. The activity of the catalyst is also negatively affected if too high a heating rate is applied (20 K min^{-1}), as illustrated for the nitrate-based catalyst in the same figure.

3.2. *Infrared spectroscopy of adsorbed NO*

To gain further information on the location and oxidation state of extraframework iron species, IR spectroscopy of adsorbed NO has been applied. Nitric oxide is a suitable probe for this study due to its strong affinity towards Fe, and because of the high intensity of the NO bands, as demonstrated by the abundant literature regarding Fe ions, both dispersed on oxidic surfaces and hosted in zeolitic matrices. In spite of the extensive literature, the assignment of the different bands of adsorbed NO on iron species is sometimes disputable [25], but nevertheless much more information on catalyst structure can be obtained with NO than with weakly adsorbed N_2O [26]. In this regard, it is worth noticing that NO is most suitable for the characterization of $Fe^{2+}(NO)_n$ rather than $Fe^{3+}(NO)_n$ complexes, because the interaction with Fe^{2+} causes a greater perturbation of the dipole moment of the adsorbed molecule, resulting in a much higher extinction coefficient of the N—O stretching in ferrous compared to ferric nitrosyls [27]. In practice, the $Fe^{3+}(NO)_n$ complexes are usually not observed.

Figure 2 shows the dynamics of the IR bands of Fe-BEA(6), the most active catalyst in this study, as a function of exposure time to the NO/He feed mixture. Clearly a band at 2160 cm^{-1}, with a shoulder at around 2193 cm^{-1} develops as a function of time. Other bands at 1874, 1850, and 1820 cm^{-1} reach there maximum intensity rather quickly. After reaching maximum intensity, only very small variations in the intensity of the 1874 cm^{-1} band occur, while the shoulder at 1850 cm^{-1} becomes more pronounced. The band at 1820 cm^{-1} grows slower, and reaches equilibration only after 5.5 min of exposure.

Figure 3 further illustrates the effect of the precursor and activation atmosphere on the spectra of NO adsorbed on the Fe(II) species in the respective catalysts. Four Fe-related bands can be observed for the catalysts Fe-BEA(1), Fe-BEA(4), Fe-BEA(5), and Fe-BEA(6) in the presence of gas-phase NO, at 1910, 1874, 1850 (shoulder), and 1820 cm^{-1}. Fe-BEA(1), prepared with the sulfate precursor and pretreated in Ar, shows the highest intensities at 1851 (shoulder) and 1819 cm^{-1}, while the 1874 cm^{-1} band is of somewhat lower intensity than the catalyst prepared with the nitrate precursor, Fe-BEA(6). In agreement with the activity data, the IR spectra of adsorbed NO on the catalysts with different precursors show only small differences in band intensities (figure 3). The Fe(III)-nitrate-based catalyst contains the highest amounts of Fe(II) sites yielding an NO absorption band at around 1875 cm^{-1}, the assignment of which will be further discussed later. The small observed differences are most likely just an effect of the small variations in Fe content of the samples.

The spectra of the sulfate and nitrate-based catalysts after pretreatment in air show significantly less intensity than after pretreatment in Ar, obviously due to the higher fraction of iron as "invisible" Fe(III) in the air-activated samples. A little less intensity of the 1874 cm^{-1} band can be observed for the oxidized sulfate-based catalyst compared to the oxidized nitrate-based catalyst. Besides the intensity differences indicated in figure 3, there is also a significant difference between the various catalysts in the rate at which the broad absorption features between 2000 and 2300 cm^{-1} increases. This is illustrated in figure 4. It is obvious that the catalysts activated in air show a very rapid initial increase, followed by a slow continuous increase, whereas for the Ar-activated catalysts a more linear increase is observed.

The effect of catalyst loading on the intensity of the NO bands is illustrated in figure 5. Again, similar absorption bands are obtained for the various nitrate-based catalysts. As expected, the catalyst containing 0.2 wt% Fe shows only very low intensity bands. However, increasing the iron content from 0.8 to 1.5 wt% Fe has no significant effect on the measured spectra.

The analysis of the various bands in the spectra in figures 2, 3, and 5 is given below. Similarities and differences will be established with respect to our previous assignments of NO absorptions on iron species hosted in steam-activated FeMFI zeolites having different framework compositions [25].

3.2.1. *Bands in the region of 2100–2200 cm^{-1}*

The origin of bands in this region has recently been discussed extensively by Hadjiivanov *et al.* [28] for an ion-exchanged Fe-ZSM-5 catalyst, as well as for H-ZSM-5. Particularly, a band at 2133 cm^{-1} is assigned to positively charged NO^+, occupying cationic positions

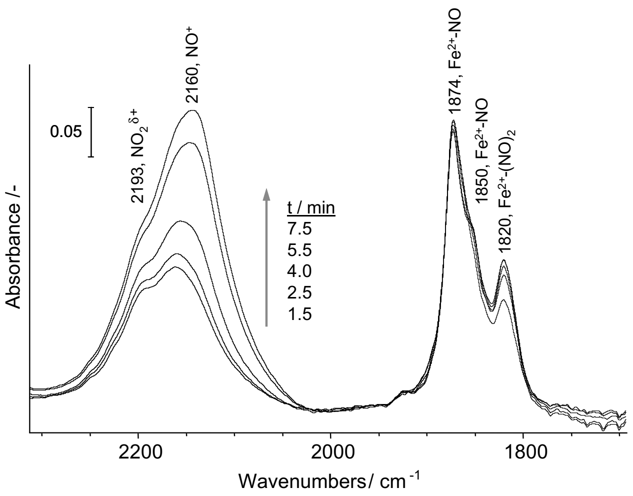

Figure 2. Evolution of DRIFT spectra of NO adsorbed on Fe-BEA(6) at 323 K in flowing 5 vol% NO/He, after pretreatment for 60 min in He at 673 K. Exposure times to the NO/He flow as indicated in the figure. Spectra are shown after subtraction of the NO gas phase spectrum.

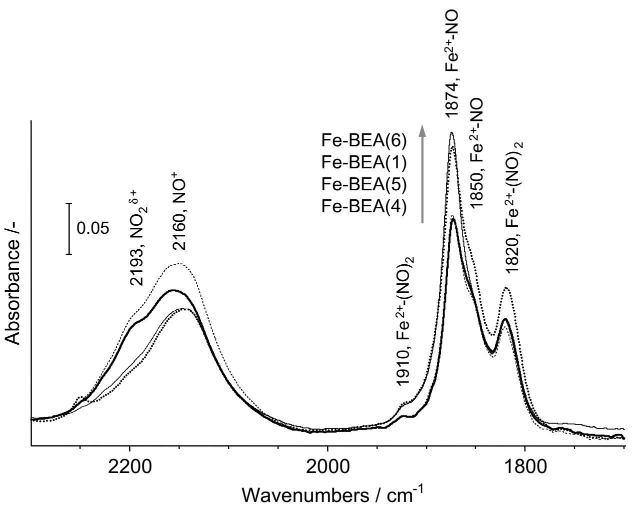

Figure 3. DRIFT spectra of NO adsorbed on Fe-BEA catalysts at 323 K in flowing 5 vol% NO/He, after pretreatment for 60 min in He at 673 K. Exposure time to the NO/He feed was 4 min. Spectra are shown after subtraction of the NO gas phase spectrum. Intensity of the 1874 cm^{-1} band in increasing order: Fe-BEA(4), Fe-BEA(5), Fe-BEA(1), and Fe-BEA(6).

in the zeolite structure. The higher wavenumber at 2195 cm^{-1} clearly observed in figure 2, has also been observed by Lobree *et al.* [29], and was tentatively assigned to some form of $NO_2^{\delta+}$. The dynamics of the intensity of the 2100–2300 cm^{-1} region for the oxidized and reduced catalysts respectively, is illustrated in figure 4. In the case of activation of the ion-exchanged Fe-BEA catalyst in air, a rapid development of the intensity of these bands is observed, and specifically a relatively high intensity of the 2195 cm^{-1} band is obtained. This suggests that NO reduces some of the oxidized Fe sites, leading to adsorbed $NO_2^{\delta+}$, while at the same time NO^+ might be formed, as suggested by Hadjiivanov *et al.* [30]. Nevertheless, the relatively low intensity of the 1874 cm^{-1} band suggests that a significant fraction of iron remains in the Fe(III) state [25].

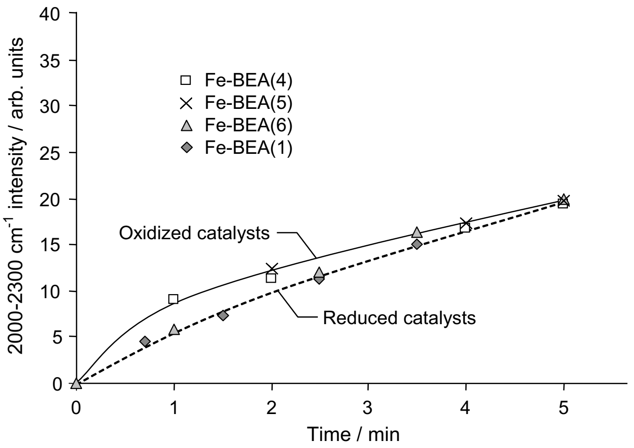

Figure 4. Intensity dynamics of 2000–2300 cm^{-1} absorption region of NO adsorbed on various Fe-BEA catalysts at 323 K in flowing 5 vol% NO/He, after pretreatment for 60 min in He at 673 K.

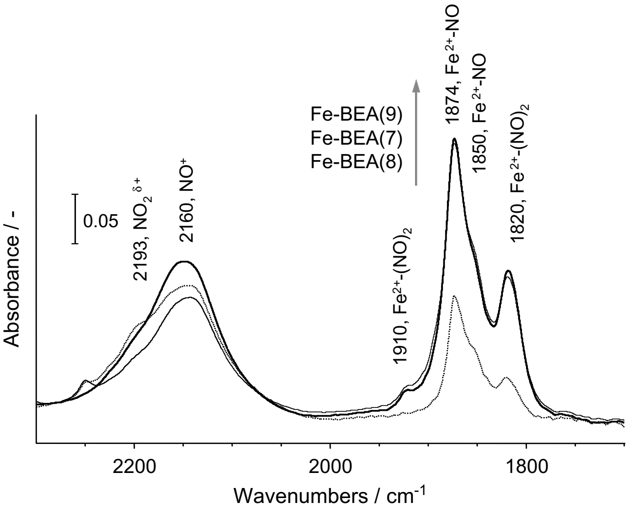

Figure 5. DRIFT spectra of NO adsorbed on Fe-BEA catalysts with different iron contents (at 323 K in flowing 5% NO/He), after pretreatment for 60 min in He at 673 K. Exposure time to the 5 vol% NO/He was 4 min. Spectra are shown after subtraction of the NO gas phase spectrum. Intensity of the 1874 cm^{-1} band in increasing order: Fe-BEA(8), Fe-BEA(7), and Fe-BEA(9).

3.2.2. *The band around 1875 cm^{-1}*

As discussed in the overview presented elsewhere [25], the single band at around 1875 cm^{-1} can be assigned to both isolated Fe(II) in specific ion exchange positions (γ-sites in ZSM-5) [31], as well as to oligonuclear Fe_xO_y clusters in the zeolite cavities [32]. Although in particular samples, e.g. steam-activated FeMFI zeolites, a doublet is observed [25], here a single peak can be fitted excellently to the absorption maximum at 1874 cm^{-1}, with a second contribution at 1853 cm^{-1}. From the significant reduction of the peak intensity shown in figure 3 for the oxygen-pretreated samples, it can be deduced that a fraction of the Fe sites remains oxidized after a He pretreatment at 673 K. As previously discussed, NO is not capable to remove oxygen from all of these sites. Hadjiivanov *et al.* [30] observed a simultaneous intensity growth of the bands at 2133 cm^{-1} (located at around 2160 cm^{-1} in our study) and at 1880 cm^{-1}, which is not identified for the FeBEA catalysts. Further analysis of the evolution of the bands at the 2160 and 1880 cm^{-1} frequencies, especially in the first minute after exposing the samples to NO, is necessary to elucidate the origin of NO^+ species in the catalytic systems.

3.2.3. The bands at 1835–1860 cm^{-1}

Bands in this region have been reported in many studies, e.g. [31,32]. Comparison of the spectra in figures 2, 3 and 5 indicates that all the samples contain the species leading to this absorption frequency, which is present as a distinct shoulder on the 1874 cm^{-1} band at around 1853 cm^{-1}. Based on the assignments of Lobree *et al.* [31] and Joyner and Stockenhuber [32] for FeZSM-5 catalysts, the 1856 cm^{-1} band can be ascribed to isolated Fe^{2+} species in ion-exchange positions of Fe-BEA. The ion-exchanged site is proposed to have an intermediate accessibility [31]. In specific cases, the intensity of the 1856 cm^{-1} band was higher, while the corresponding activity of the particular catalyst was lower (figure 3). This suggests that the Fe-species responsible for this NO absorption is not very important for the N_2O decomposition catalysis.

3.2.4. The band at 1800–1820 cm^{-1}

A second quite predominant band in the various spectra is located at around 1820 cm^{-1}, which shows much less stability than the absorption at 1874 cm^{-1}. For ZSM-5 based catalysts, several authors have assigned this band to dinitrosyls on isolated Fe ions in relatively highly accessible channels of the zeolite (the other band is located around 1920 cm^{-1}), with the corresponding band of the mononitrosyl at around 1765 cm^{-1} [30,31]. On the other hand, Joyner and Stockenhuber [32] assigned this band to a dinitrosyl on an iron oxidic cluster, based on an intensity correlation between the 1880 cm^{-1} band and the 1815 cm^{-1} band for four different samples at similar NO pressure. Clearly, the spectra shown in figure 2 indicate that for Fe-BEA no correlation exists been the 1874 and 1820 cm^{-1} bands, which was confirmed by evaluation of the bands after band fitting. At the same time, the 1765 cm^{-1} has never been observed if the gas phase was changed to He, while this led to a decreased intensity of the 1820 cm^{-1} band (not shown). Therefore, either the 1820 cm^{-1} band has to be assigned to a mononitrosyl species on a specific site in the BEA zeolite, or the mononitrosyl desorption rate is faster than the conversion of the dinitrosyl into the mononitrosyl species; i.e. there is an apparent direct decomposition of the dinitrosyl into two molecules of NO in the gas phase, without forming the corresponding mononitrosyl. Whichever the reason, the most important conclusion from the present study, is that no correlation between the intensity of this absorption band and N_2O decomposition activity was found.

4. Discussion

4.1. Role of preparation variables in N_2O decomposition activity

From the results presented above, it appears that heat treatment of the catalyst precursor obtained after filtration and washing, significantly affects the performance of the catalysts obtained. Both, Kameoka *et al.* [22,23], and Mauvezin *et al.* [19] used air treatment to prepare the final catalytic material. It was demonstrated by Delahay *et al.* [20] using TPD experiments, that iron-oxo species generated by calcination of Fe^{2+}-BEA in air are relatively stable compared to those formed upon reoxidation by nitrous oxide. It is thus likely that an irreversible oxidation of a fraction of the Fe-sites important in N_2O decomposition has occurred. Apparently auto-reduction of these sites by pretreatment in He at 673 K, the standard procedure before activation data were collected, is not possible. The differences in activity correlate with intensities observed in the IR spectra in figure 3. The contribution of Fe^{3+} sites to the spectra of adsorbed NO is very low, if anything at all [25], confirming that a significant fraction of Fe in the air-activated samples is in an inactive Fe(III) state, even after He pretreatment at 673 K.

As it was demonstrated in figure 1c, a high heating rate in argon is also diminishing the performance of the catalyst in N_2O decomposition. An extensive study was described by Battiston *et al.* [13], on the effect of the pretreatment conditions on the constitution of Fe-ZSM-5 catalysts prepared by sublimation. These authors found that high heating rates induce clustering of the Fe sites as a result of a high water concentration in the catalyst activation reactor. In line with this hypothesis, clustering to inactive species also appears the explanation for the lower activity in direct N_2O decomposition of the catalyst pretreated with a heating rate of 20 K min^{-1}, which is in agreement with the lower IR absorption intensity of adsorbed NO at around 1875 cm^{-1}.

In agreement with the observation of Coq *et al.* [19,20], the present manuscript indicates that the amount of Fe optimizes, and that too high a loading diminishes the activity. Various papers have appeared that discuss the effect of the iron content on the structure and performance of Fe-zeolite catalysts. Generally, it was observed that at high ion-exchange levels, large Fe_2O_3 particles are formed, besides the catalytically active species in the zeolite channels [19,20,29,31]. The origin of the catalytic activity in the various reactions catalyzed by Fe-zeolites has been intensively debated over the last decade. Despite considerable efforts to characterize these materials, particularly the FeZSM-5 system, available data are not yet sufficient to conclude exclusively on the active form(s) of iron. Binuclear iron species in FeZSM-5 have been designated as the active site in various reactions, including selective oxidation of benzene to phenol with N_2O, direct N_2O decomposition, and SCR of NO_x with hydrocarbons [4,33,34]. However, in the last reaction, small oligonuclear species of composition Fe_4O_4 [32] and isolated iron ions [14] have also been proposed as active sites. Although we have not performed an extensive characterization of the iron species by multiple techniques, some aspects of the active iron site for N_2O decomposition will be discussed in the following, based on a correlation between activity and IR intensities of adsorbed NO species at 1874 cm^{-1}.

4.2. Correlation between IR bands and N_2O decomposition activity

In figure 6, a correlation is shown between the intensity of the 1874 cm^{-1} band (in Reflectance Absorbance units) and the conversion determined in the activity measurements at 693 K over different Fe-BEA catalysts. It is fair to state that a good correlation exists. Hence, it can be concluded that the species causing the 1874 cm^{-1} NO absorption band is very important for N_2O decomposition. As discussed in Section 3.2, only Fe(II) species in the zeolite can be probed by NO. Thus the obtained correlation does not account for active Fe(III) species. Using various spectroscopic techniques, several groups have shown the dramatic reduction of Fe(III) to Fe(II) upon thermal activation of Fe-silicalite and FeZSM-5 in vacuum or steam [34,35]. According to Panov *et al.* [34,36], these Fe^{2+} sites play a dominant role in alpha-site formation, and should be therefore connected to the remarkable catalytic properties of FeZSM-5 in the selective oxidation of benzene to phenol with N_2O. The correlation obtained here also suggests that ferrous ions play an important role in the catalyst activity and thus makes FT-IR of adsorbed NO a very suitable technique to identify structure–activity relationships in reactions catalyzed by iron zeolites.

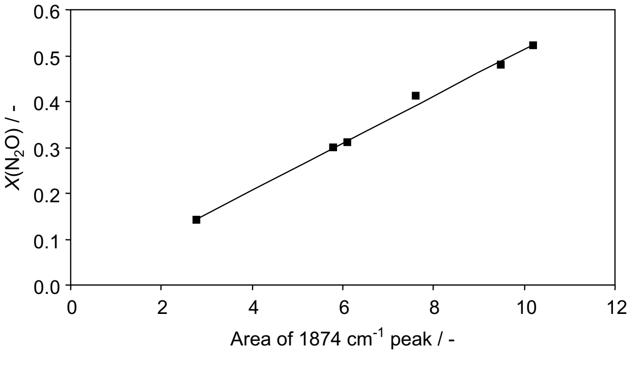

Figure 6. Intensity correlation between the 1874 cm^{-1} NO absorption band (conditions as in figures 3 and 5) versus N_2O conversion at 693 K on various Fe-BEA catalysts (conditions as in figure 1).

Two mechanisms have been typically proposed for N_2O decomposition, in which oxygen recombination is involved (equations (1a) and (b)), or direct reaction of N_2O with the oxidized site (equations (2a) and (b)):

$$2N_2O + 2^* \rightarrow 2N_2 + 2O^* \quad (1a)$$

$$2O^* \rightarrow O_2 + 2^* \quad (1b)$$

$$N_2O + {}^* \rightarrow N_2 + O^* \quad (2a)$$

$$N_2O + O^* \rightarrow N_2 + O_2 + {}^* \quad (2b)$$

Two neighboring Fe-sites would favor the recombination of two adsorbed O^* atoms originating from N_2O, to generate O_2. If mechanism (1a–b) is prevailing, this suggests that the 1874 cm^{-1} band is related to Fe_xO_y clusters, as was proposed by Joyner and Stockenhuber [32]. These authors applied X-ray absorption spectroscopy and concluded an average composition of Fe_4O_4 for such oligomers. On the other hand, if mechanism (2a–b) is dominant, also an isolated Fe-site might be the active site, and an interpretation of the 1874 cm^{-1} band to NO adsorbed on isolated sites is feasible. A transient study using Multitrack, an advanced TAP (Temporal Analysis of Products) reactor, provided evidence that mechanism 1 occurs in a wide temperature range (698–823 K) over steam-activated FeZSM-5 [37,38]. Below 698 K the catalyst activity was very low, and no O_2 was measured by the different mass spectrometers at the TAP reactor exit. More recently, using a number of FeMFI catalysts with different nature and distributions of iron species, a correlation between the desorption of molecular oxygen from the TAP microreactor (upon pulsing N_2O), the activation energy of O_2 formation in steady-state kinetic studies at N_2O conversions <5%, and the catalytic activity for N_2O decomposition has been established [J. Pérez-Ramírez, in preparation]. Furthermore, a sample with a uniform distribution of iron species as extraframework iron ions in isolated positions resulted in significantly less active direct N_2O decomposition as compared to clustered iron-zeolites [16]. This strongly supports that iron association in the form of oligonuclear species favors desorption of molecular oxygen, which is the rate-determining step. Moreover, this confirms that the 1874 cm^{-1} band is related to Fe_xO_y clusters in BEA zeolite. Still, the authors propose further research in the area of N_2O decomposition over Fe-zeolite catalysts, e.g. to understand the results of Nobukawa *et al.* [39], who have stated that mechanism 2 is predominant over FeMFI using an ^{18}O-tracer technique.

5. Conclusions

The most important finding of the present contribution is that a correlation exists between the absorption intensity of adsorbed NO on oligonuclear ferrous $Fe_x^{2+}O_y$ clusters in the BEA zeolite at 1874 cm^{-1}, and the activity of the catalysts in N_2O decomposition. This correlation was obtained by adjusting preparation variables. An optimal iron loading for N_2O decomposition of 0.8 wt% Fe was found, with no significant influence of the used Fe-precursor. Activation of the ion-exchanged catalysts in inert yields significantly better performance than activation in air. The observed relationship can be used as a reliable and fast assessment of catalyst performance for Fe-BEA zeolites in direct N_2O decomposition.

Acknowledgments

This research was financially supported by the Dutch Council for Chemistry Research (CW-NWO). Fruitful discussions with Dr. R.W. van den Brink and Dr. J.A.Z. Pieterse (ECN) are appreciated by the authors. G.M. gratefully acknowledges a fellowship granted by the Royal Netherlands Academy of Arts and Sciences.

References

[1] J. Pérez-Ramírez, G. Mul, F. Kapteijn and J.A. Moulijn, Chem. Commun. (2001) 693.
[2] J. Pérez-Ramírez, F. Kapteijn, X. Xu, G. Mul and J.A. Moulijn, Catal. Today 76 (2002) 55.
[3] J. Pérez-Ramírez, F. Kapteijn, K. Schöffel and J.A. Moulijn, Appl. Catal. B. 44 (2001) 117.
[4] H.-Y. Chen and W.M.H. Sachtler, Catal. Lett. 50 (1998) 125.
[5] C. Pophal, T. Yogo, K. Yamada and K. Segawa, Appl. Catal. B. 16 (1998) 117.
[6] B. Coq, M. Mauvezin, G. Delahay, J.B. Butet and S. Kieger, Appl. Catal. B. 27 (2000) 193.
[7] R.Q. Long and R.T. Yang, Chem. Commun. (2000) 1651.
[8] G.I. Panov, V.I. Sobolev and A.S. Kharitonov, J. Mol. Catal. 61 (1990) 85.
[9] A. Ribera, I.W.C.E. Arends, S. de Vries, J. Pérez-Ramírez and R. Sheldon, J. Catal. 195 (2000) 287.
[10] J. Pérez-Ramírez and E.V. Kondratenko, Chem. Commun. (2003) 2152.
[11] R.Q. Long and R.T. Yang, Catal. Lett. 74 (2001) 201.
[12] K. Krishna, G.B.F. Seijger, C.M. van den Bleek, M. Makkee, G. Mul and H.P. Calis, Catal. Lett. 86 (2003) 121.
[13] A.A. Battiston, J.H. Bitter, F.M.F. de Groot, A.R. Overweg, O. Stephan, J.A. van Bokhoven, P.J. Kooyman, C. van der Spek, G. Vanko and D.C. Koningsberger, J. Catal. 213 (2003) 251.
[14] F. Heinrich, C. Schmidt, E. Löffler, M. Menzel and W. Grünert, J. Catal. 212 (2002) 157.
[15] J. Pérez-Ramírez, F. Kapteijn, J.C. Groen, A. Doménech, G. Mul and J.A. Moulijn, J. Catal. 214 (2003) 33.
[16] J. Pérez-Ramírez, F. Kapteijn and A. Brückner, J. Catal. 218 (2003) 234.
[17] M. Mauvezin, G. Delahay, F. Kisslich, B. Coq and S. Kieger, Catal. Lett. 62 (1999) 41.
[18] B. Coq, M. Mauvezin, G. Delahay and S. Kieger, J. Catal. 195 (2000) 298.
[19] M. Mauvezin, G. Delahay, B. Coq, S. Kieger, J.C. Jumas and J. Olivier-Furcade, J. Phys. Chem. B. 105 (2001) 928.
[20] G. Delahay, M. Mauvezin, B. Coq and S. Kieger, J. Catal. 202 (2001) 156.
[21] G. Delahay, M. Mauvezin, A. Guzmán-Vargas and B. Coq, Catal. Commun. 3 (2002) 385.
[22] S. Kameoka, K. Kita, T. Takeda, S. Tanaka, S. Ito, K. Yuzaki, T. Miyadera and K. Kunimori, Catal. Lett. 69 (2000) 169.
[23] S. Kameoka, K. Kita, S. Tanaka, T. Nobukawa, S. Ito, K. Tomishige, T. Miyadera and K. Kunimori, Catal. Lett. 79 (2002) 63.
[24] J. Pérez-Ramírez, R.J. Berger, G. Mul, F. Kapteijn and J.A. Moulijn, Catal. Today, 63 (2001) 93.
[25] G. Mul, J. Pérez-Ramírez, F. Kapteijn and J.A. Moulijn, Catal. Lett. 80 (2002) 129.
[26] B.R. Wood, J.A. Reimer and A.T. Bell, J. Catal. 209 (2002) 151.
[27] G. Berlier, A. Zecchina, G. Spoto, G. Ricchiardi, S. Bordiga and C. Lamberti, J. Catal. 215 (2003) 264.
[28] K. Hadjiivanov, J. Saussey and J.C. Lavalley, Catal. Lett. 52 (1998) 103.
[29] L.J. Lobree, I.C. Hwang, J.A. Reimer and A.T. Bell, Catal. Lett. 63 (1999) 233.
[30] K. Hadjiivanov, H. Knözinger, B. Tsyntsarski and L. Dimitrov, Catal. Lett. 62 (1999) 35.
[31] L.J. Lobree, C.M. Hwang, J.A. Reimer and A.T. Bell, J. Catal. 186 (1999) 242.
[32] R.W. Joyner and M. Stockenhuber, J. Phys. Chem. B. 103 (1999) 5963.
[33] El.-M-El-Malki, R.A. van Santen and W.M.H. Sachter, J. Catal. 196 (2000) 212.
[34] K.A. Dubkov, N.S. Ovansesyan, A.A. Shteinman, E.V. Starokon and G.I. Panov, J. Catal. 207 (2002) 341.
[35] A. Zecchina, S. Bordiga, G. Spoto, A. Damin, G. Berlier, F. Bonino, C. Prestipino, and C. Lamberti, Top. Catal. 21 (2002) 67.
[36] E.V. Starokon, K.A. Dubkov, L.V. Pirutko and G.I. Panov, Top. Catal. 23 (2002) 137.
[37] J. Pérez-Ramírez, F. Kapteijn, G. Mul and J.A. Moulijn, J. Catal. 208 (2002) 211.
[38] G. Mul, J. Pérez-Ramírez, F. Kapteijn and J.A. Moulijn, Catal. Lett. 77 (2001) 7.
[39] T. Nobukawa, S. Tanaka, S. Ito, K. Tomishige, S. Kameoka and K. Kunimori, Catal. Lett. 83 (2002) 5.